

The Development of a Submm-Wave Uncooled Bolometric System and Field Test

Roberto R. Neli, Arline M. Melo, Cristiano J. N. Arbex, Maria B. P. Zakia, Ioshiaki Doi, Pierre Kaufmann, Jacobus W. Swart and Edson Moschim.

Abstract - Developments directed to potential interest for telecommunications in the submillimeter and far infrared wavelengths band have been increasing in recent years. The detection of radiation in that spectral region has various other important applications in remote passive radiometric sensing, some times called as thermosensing, such as imaging of field targets, power line surveys, night vision, radio meteorology, atmospheric propagation and astrophysics. The development of a non-imaging bolometer detector for incoherent radiation in the submillimeter bands is presented. Construction details are presented for a detector's active material using polycrystalline and amorphous silicon. We describe the bandpass filters to be placed in front of the detector, which are being designed to be constructed using the resonant mesh technology, centered at the peak frequencies around 405, 670 and 850 GHz. The bolometric system will be submitted to qualification and performance tests at the focal plane of a 1.5-m submillimeter reflector located at a high altitude dry site (El Leoncito, Argentina Andes), using the Sun as a source of blackbody radiation, and a beacon transmitter at 405 GHz located in the far field with respect to the reflector. The first applications considered for the system are measurements of atmospheric propagation, solar imaging and tentative detection of solar transients (flares) in the selected bands.

Resumo - Nos últimos anos tem se dado crescente importância ao desenvolvimento de microbolômetros, atendendo interesses potenciais para telecomunicações, da faixa submilimétrica ao infravermelho distante. A detecção de radiação nesta

Roberto R. Neli is a doctoral graduate student at CCS – FEEC, Unicamp, Campinas SP, Brazil.

Arline M. Melo is a MS graduate student at CCS – FEEC, Unicamp, Campinas SP, Brazil and stays part time at CRAAM – Universidade Presbiteriana Mackenzie, São Paulo, SP, Brazil;

Cristiano J. N. Arbex is a MS graduate student at CCS – FEEC, Unicamp, Campinas SP, Brazil;

Maria Beny is full-time researcher at CCS – Unicamp, Campinas, SP, Brazil;

Ioshiaki Doi, is a professor at FEEC-Unicamp and Vice-Director of CCS – Unicamp, Campinas, SP, Brazil;

Pierre Kaufmann is professor at CRAAM - Universidade Presbiteriana Mackenzie, São Paulo, SP, Brazil and part-time researcher at CCS – Unicamp, Campinas, SP, Brazil;

Jacobus W. Swart is professor at FEEC and Director of CCS – Unicamp, Campinas, SP, Brazil;

Edson Moschim is professor at FEEC, Unicamp, Campinas, SP, Brazil;

This research is being partially supported by FAPESP, Brazil, contracts 99/06126-7 and 02/04774-6, CNPq contracts 690190/02-6 and 140583/02-5, CAPES for CJNA master course fellowship, and by

CONICET.

região espectral tem várias outras importantes aplicações em sensoriamento passivo remoto, também chamado de termosensoriamento, tais como imageamento de alvos no campo, supervisão de redes elétricas de potência, visão noturna, rádio meteorologia, propagação atmosférica e astrofísica. Este trabalho apresenta o desenvolvimento de um detector bolométrico, não imageador, de radiação incoerente em bandas submilimétricas, bem como os testes de campo previstos. São apresentados detalhes de construção do material ativo, formado por silício policristalino ou amorfo, do detector utilizando.

Descrevemos os filtros passa-banda a serem instalados frente o coletor de fótons e o detector, projetados e construídos para frequências centradas em 405, 670 e 850 GHz. O sistema bolométrico será submetido a testes de qualificação e de desempenho no plano focal de um refletor submilimétrico de 1,5m localizado em sítio seco de elevada altitude (El Leoncito, Andes Argentinos), usando o Sol como fonte de radiação com característica de corpo negro, e um transmissor artificial de 405 GHz localizado à distância remota com relação ao refletor. Como primeiras aplicações consideradas para o sistema estão medidas de propagação atmosférica, imageamento solar, e detecção tentativa de transientes solares (explosões) nas bandas

Index Terms—Infrared detectors, submillimeter transmission, silicon devices, bandpass filters, bolometers.

I. INTRODUCTION

The detection of non-coherent electromagnetic waves in the range that includes millimetric, submillimetric waves until the far-infrared, uses bolometers or microbolometer array sensors which have their electric characteristics changed by the incidence of electromagnetic radiation.

In this project we will use resistive bolometers, where their electric resistance modifies when the radiation is absorbed. Their basic structure consists of a fine film of metal or semiconductor with an absorber film placed above, usually suspended by a substrate producing a thermal isolation (Fig. 1).

The detectors used in the submm-wave – IR range can be cooled or not. In more recent years uncooled detectors have been widely used. They provide good sensitivity at room temperature bringing advantages like low cost, low weight and low power consumption.

Among the various applications for the detectors that operate in these high frequencies there is an important potential future for telecommunications, from the ground in the range where there are atmospheric “windows” for transmission and above the Earth’s troposphere for communications between platforms (balloons, airplanes and stationary devices) or between satellites.

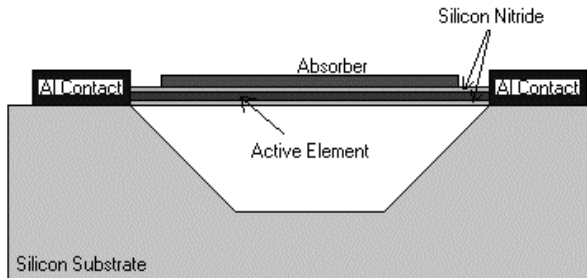


Fig. 1. Microbolometer Structure.

Other important applications to be mentioned are the passive imaging made through clouds, fog, rain, smoke and even through walls; devices that allow night vision; terrestrial mining detection; fire detection; security devices; cameras for medical and industrial applications; mine sensors in battlefields for military purposes. Several thermosensing applications have been developed for agriculture, ground and crops surveys [Refs. 1-3].

This range of the electromagnetic spectrum is also of a great interest for space sciences, because it brings essential spectral information on the cosmic background radiation, on distant galaxies recently formed and on the initial phases of stellar formation in gas clouds in our own galaxy [4].

The diagnostics of astrophysical objects in the submm-IR range – with emphasis to the Sun - not only in the continuum but also in spectral lines; are in the front line of current research. In this range of wavelengths it is possible to distinguish thermal from the non-thermal emissions caused by relativistic particles. These measurements can be developed from the ground, or from space platforms in balloons and satellites.

The design of a room-temperature bolometric detection system has been developed, which basic technical features, qualification tests, and first applications are described here.

II. DEPOSITION AND PROCESSING PARAMETERS

An alternative way to perform thermally insulated bolometers consists of micromachining the active element to form a microbridge which is anchored to the silicon substrate through thin supports. The thermal detectors are based on the effect of temperature change caused by the heat absorbed from incident radiation upon the detector [5]. They have a number of advantages including wide spectral response, room temperature operation and low cost. The thermal insulation is determined by the geometry and the thermal conductivity of the supports. Strong candidates for the active material to be used are poly and amorphous silicon. Their electrical temperature

coefficient of resistance and conductivity (TCR) can be easily controlled by boron doping. It is fully compatible with integrated circuit (IC) technology, can operate in a wide range of temperature and presents low cost technology.

Using silicon anisotropic etching in potassium hydroxide solution (KOH, 10M at 82°C), various shapes of bridges were fabricated as shown in Fig. 2.

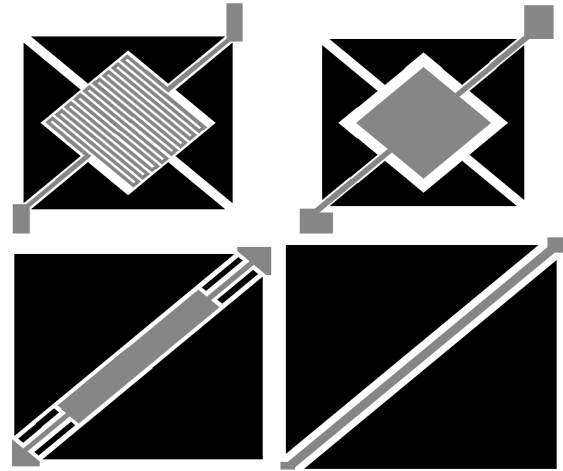


Fig. 2. Shapes of Bridges.

Nitride silicon or silicon oxide films are prepared on a (100)-oriented silicon substrate as support films acting as microbridges. First, the silicon wafer has been covered with a 500nm silicon nitride deposited by electron synchrotron resonance (ECR), or with a 1µm silicon oxide, grown in a wet oxidation. In the following step, a 1µm thick poly or amorphous silicon layer is deposited on top of silicon nitride using chemical vapor deposition (CVD). The silicon nitride layer is implanted with a low boron dose ($3 \times 10^{13} \text{ B cm}^{-2}$) in order to obtain the desired resistivity and TCR. A 100 nm thick layer of silicon nitride is deposited onto poly silicon in order to insulate the submm-wave/infra-red absorber from the active element [6]. These three layers consist the pattern in order to define the support legs and active area, whereas the support legs are highly doped ($10^{16} \text{ B cm}^{-1}$) [7], to act as electrical contacts. This highly doping also forms a *p-n* junction with silicon substrate proving an electrical insulation. After deposition of metal contacts, the processing of the absorber formed by a porous gold layer.

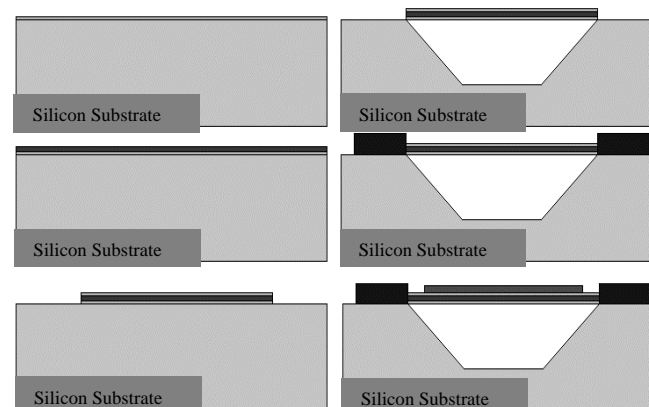


Fig. 3. Schematic flow chart of silicon microbolometers

fabrication.

This layer is known as “gold black” or “gold soot” and is obtained by gold evaporation in nitrogen atmosphere. [8]. The absorber function is to convert the incident radiation into heat. It must have high absorption efficiency, high reproducibility and must be compatible with standard process. We can observe a bolometer fabrication scheme in Fig. 3.

III. RESONANT MESH AS BANDPASS FILTERS

There are many applications for bandpass filters in the submm-wave to far-infrared range of frequencies. For example, “tunnel” junction mixers need bandpass filters to avoid the saturation by thermal radiation [9]. The noise equivalent power of a bolometer can also be reduced by using a bandpass filter to block the thermal radiation over the spectral range of the detector [9].

Bandpass filters are used in bolometric systems to select spectral frequencies of non-coherent electromagnetic waves in the range that includes millimetric, submillimetric extending to the far-infrared waves, on various applications in passive sensing or imaging. In the present case, the filters designs must have center frequencies to fit the atmospheric transmission windows, similarly to the selections made by Chase and Joseph [10]. Such filters should present good transmission at the center of the band and excellent blocking for lower and higher frequencies.

There is a variety of resonant mesh structures with different shapes that produce bandpass response, such as arrays of crosses; arrays of circular and square conducting rings and pairs of concentric circular conducting rings [Ref. 9-12]. Our attention will be directed to arrangements of cross-shaped elements.

It is known that a conductive plate with a square opening acts as a high-pass filter, and in the transmission lines model context is considered as an inductive arrangement [10,11].

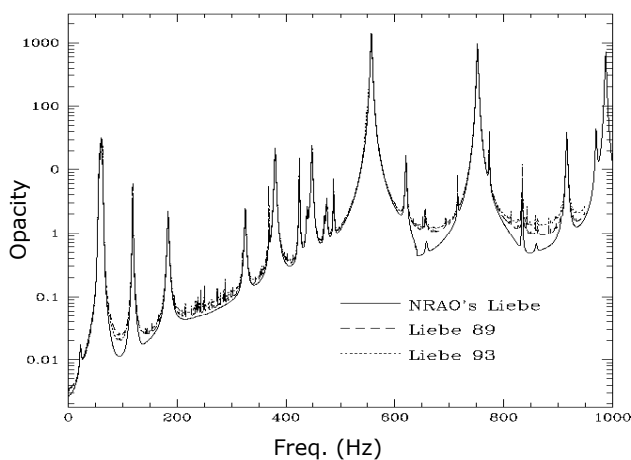


Fig. 4. Atmospheric opacity (in nepers) vs. frequency (in GHz).

Similarly, an arrangement with a complementary structure, acts as a low-pass filter also called as a capacitive arrangement.

Associating those two arrangements, a bandpass behavior is obtained, as is the case of the cross-shaped elements arrangement [11]. Considering typical atmospheric spectral transmission characteristic [Refs. 13-16], we selected transmission “windows” centered in the frequencies around 405, 670 e 850 GHz for the filters.

These frequencies correspond, to the following wavelengths: 741 μm, 448 μm and 352 μm, respectively as we can see in Fig. 4. The design parameters were studied for bandpass filters centered on those bands.

Several authors have used cross-shaped elements as bandpass filters with different notations to characterize the crosses’ dimensions [Refs. 9-11]. In this work we will follow the nomenclature given by Chase and Joseph [10]. The cross-shaped elements have the design shapes shown in Fig. 5, where g is the periodicity, L is the cross length, $2b$ is the cross width and $2a$ is the separation between crosses.

$$g = L + 2a \tag{1}$$

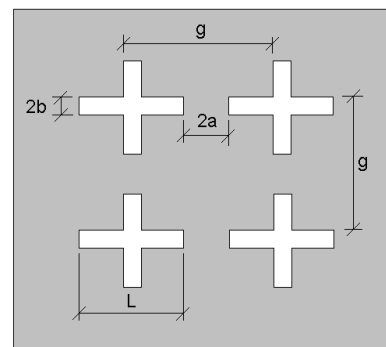


Fig. 5. Definition of the cross-shaped mesh parameters.

The resonance wavelength (wavelength where occurs the maximum transmission) is given by [10,12]:

$$\lambda_0 = 2.LL \tag{2}$$

on the condition that the b/a ratio is smaller than 1.

Thus, for each value of the filter central frequency, there are corresponding values for L , close to a half-wavelength.

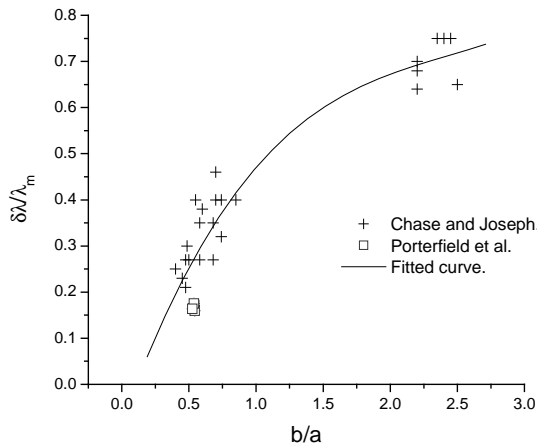


Fig. 6. Measured data and fitted curve for the bandwidth vs b/a ratio.

For 220 GHz, we obtain $L = 649 \mu\text{m}$. For 410 GHz, $L = 348 \mu\text{m}$ and for 670 GHz, $L = 213 \mu\text{m}$. Our design looks for a small bandpass, nearly 25% of the central wavelength. Fig. 6 shows the dependence of the bandwidth with the b/a ratio. The experimental data were obtained from Porterfield et al. [9] and Chase and Joseph [10]. Fitting the data of Fig. 6 derived an empirical equation relating the bandpass and the b/a ratio:

$$\frac{\delta\lambda}{\lambda_m} = -0.0839 + 0.8115\left(\frac{b}{a}\right) - 0.2984\left(\frac{b}{a}\right)^2 + 0,0409\left(\frac{b}{a}\right)^3 \quad (3)$$

where using $\delta\lambda/\lambda_m = 0.25$, we get $b/a \cong 0.5$.

IV. THE CONSTRUCTION OF FILTERS

Using the Eq.1 and Eq.2, adopting g equal 80% of the resonant wavelength $g = 0.8 \lambda_0$ and $b/a \cong 0.5$ as the result of the Eq.3, the following filter parameters are obtained:

| f (GHz) | g (μm) | L (μm) | a (μm) | b (μm) |
|---------|--------|--------|--------|--------|
| 220 | 1091 | 649 | 221 | 111 |
| 410 | 586 | 348 | 119 | 60 |
| 670 | 358 | 213 | 73 | 37 |

The filter construction is being considered with the use of photolithography process associated to an etching process or metal deposition. Porterfield et al. [9] uses the copper electroplating process for the crosses formation. Initially a thin copper layer is deposited on a glass substrate. Then, photoresist is applied on the whole copper surface which is submitted to exposure to UV followed by the photoresist development, so that the crosses become in high relief. Then the copper electroplating around the photoresist crosses is done. Removing the photoresist produces the crosses cavity. The initial copper layer is removed with a light etching.

Chase and Joseph [10] and Tomaselli et al. [11] used the etching process to obtain the mesh crosses. In this process a metal substrate (aluminum [12] or copper [11])

is deposited onto a thin Mylar substrate. After the photoresist is applied the exposure is done. Later, the metal etching is accomplished to obtain opaque crosses.

MacDonald et al. [12] uses the liftoff process. A polyester substrate is glued with photoresist on a base formed by a silicon substrate. The polyester is covered with photoresist to perform the exposure and development, so that the crosses become in high relief. A gold or lead layer is later deposited by sputtering, so that the cross is surrounded by metal. Acetone can be used to remove the polyester of the substrate.

For the present design we will consider the processes described by Porterfield et al. [9], Chase and Joseph [10] and Tomaselli et al. [11].

Fig. 7 illustrates two enlarged views of a 565 GHz mesh filter built in the CCS laboratory for bandpass testing purposes.

The complete bolometric system will be assembled at the end of a “photon trap” to achieve maximum collection of radiation using the technique of non-imaging concentrator, also known as Winston cone [17] [18].

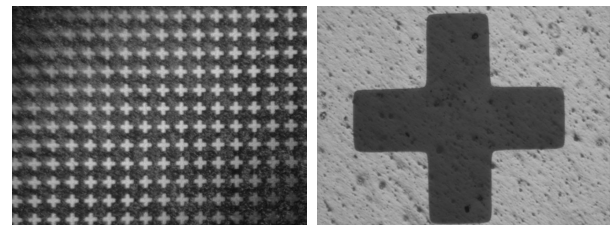


Fig.7. Enlarged views of resonant mesh filter designed for center frequency of 565 GHz, built on aluminum/plastic film at CCS laboratory.

V. OBJECTIVES AND TESTS

This project proposes the establishment of definitions, prototype construction and installation of a bolometric system in the focal plane of a 1.5-m reflector for submm-waves (SST project) installed in Argentina Andes [19] – which was made available for the present research. The assembly will be used

Fraction of observing time

Fraction of observing time

Daytime atmospheric opacity at 212

Daytime atmospheric opacity at 405

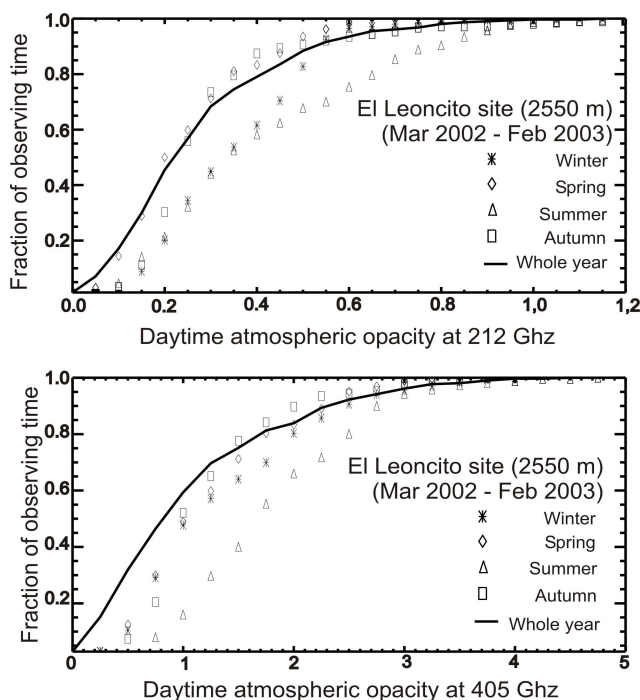


Fig. 8. The cumulative opacity plots for El Leoncito for 212 GHz (top) and 405 GHz (bottom) for one year of measurements [17,18].

for tests on its performance, radiation detection, and qualification. Solar emission will be used as a source of continuum radiation, exhibiting a black body spectrum. At one frequency band, 0.4 THz, a beacon transmitter will be used at the same site, located in the far field with respect to the reflector.

Recent measurements of atmospheric opacity for the site of El Leoncito show that nearly 60% of the observing time has opacities smaller than 0.35 (Nepers) for 212 GHz and 1.5 (Nepers) for 405 GHz, showed in Fig. 8. This study was made for measurements during one year of observations (Mar 2002 -Feb 2003) [20] [21]. According to model predictions [Refs. 13-16] the fraction of observing time for an atmospheric opacity smaller than 2.0 (Nepers) at 670 GHz and 850 GHz at El Leoncito is expected to be in the range of 50 - 70 %, therefore nearly 170 days in a year.

A number of applications are also being considered for this initial phase. They will concentrate on atmosphere propagation, which inhomogeneities and opacity determinations are not very well known in this range of frequencies [13], as well as on solar imaging and possible solar transients detections (flares). These measurements will complement the works that are been done at submm-waves propagation using SST at frequencies for which there are coherent heterodyne radiometers available (212 and 405 THz).

VI. FINAL REMARKS

It has been shown that submm-wave-far IR uncooled sensors using resistive bolometers can be used to perform high frequency measurements of uncoherent radiation in

various applications. A small bias is generated when submm-infrared radiation from the emitting source is directed to the detector, measured by an external circuit. Poly and amorphous silicon can be used as active element built in different patterns which will be measured to observe the best result. The resistivity and TCR of the active element can be obtained by ion implantation and low-temperature annealing. The microbolometer was coupled to a submm-IR absorber with low thermal mass, forming in this way an efficient bolometer. Bandpass filters using resonant mesh technology will be used to limit the operation frequency band, defining the spectral resolution of the measurements. We selected atmospheric transmission windows to centralize the frequencies 400, 670 and 850 GHz for the filters designs. The complete process for their fabrication was described. Performance and qualification tests will be performed placing the bolometer system in the focal plane of a 1.5-m submm-wave reflector, located in a high and dry mountain site (El Leoncito, San Juan, Argentina). Solar black body emission will be used as a test radiation source for the three bands, together with a 410 GHz far field beacon transmitter at the same site. Initial applications will be directed to atmospheric transmission measurements, solar imaging and transient detection.

REFERENCES

- [1] D. S. Tezcan, T. Akin, "A CMOS N-well Microbolometer FPA with Temperature Coefficient Enhancement Circuitry," SPIE 4369, 240-249, 2001.
- [2] D. Murphy, M. Ray, R. Wyles, J. Asbrock, N. Lum, A. Kennedy, J. Wyles, C. Hewitt, G. Graham, W. Radford, J. Anderson, D. Bradley, R. Chin, T. Kostrzewa, "High sensitivity (25 μm pitch) microbolometer FPAs and application development", SPIE 4369, 223-234, 2001.
- [3] O. Savry, P. Agnès, "Arrays of bolometer detector for millimeter wave imaging: feasibility, performances and construction of a prototype," Présenté à IRMMW Toulouse, 2001.
- [4] T. G. Phillips, "Techniques of submillimeter astronomy", Millimetre and Submillimetre Astronomy, vol. 147, pp. 1-25, 1988.
- [5] L. Dobrzanski, E. Nossarzewska-Orlowska, Z. Nowak, J. Piotrowski, "Micromachined silicon bolometers as detectors of soft X-ray, ultraviolet, visible and infrared radiation," Sensors and Actuators A, vol. 60, pp. 154-159, 1997.
- [6] S. Sedky, P. Fiorini, M. Cayamax, A. Verbist and C. Baert, "IR bolometers made of polycrystalline silicon germanium," Sensors and Actuators A, vol. 66, pp. 193-199, 1998.
- [7] T. A. Core, W. K. Tsang, S. J. Sherman, "Fabrication technology for an integrated surface-micromachined sensor," Solid State Technology, vol. 36, 1993.
- [8] S. J. Lee, Y. H. Lee, S. H. Suh, Y. J. Oh, T. Y. Kim, M. H. Oh, C. J. Kim, B. K. Ju, "Uncooled thermopile infrared detector with chromium oxide absorption

- layer," *Sensors and Actuators A*, vol. 95, pp. 24-28, 2001.
- [9] D. W. Porterfield, J. L. Hesler, R. Densing, E. R. Mueller, T.W. Crowe, and R. M. Weikle II, "Resonant metal-mesh bandpass filters for the far infrared," *Appl. Opt.*, vol. 33, no. 25, pp. 6046-6052, Sept. 1994.
- [10] S.T. Chase and R. D. Joseph, "Resonant Array bandpass filters for the far infrared," *Appl. Opt.*, vol. 22, no. 11 pp. 1775-1779, June 1983.
- [11] V. P. Tomaselli, D. C. Edewaard, P. Gillan, and K. D. Möller, "Far-infrared bandpass filter from cross-shaped grids," *Appl. Opt.*, vol. 20, no. 8, pp. 1361-1366, April 1981.
- [12] M. E. MacDonald, A. Alexanian, R. A. York, Z. Popovic, and E. Grossman, "Spectral transmittance of lossy printed resonant-grid terahertz bandpass filters," *IEEE Trans. Microwave Theory and Techniques*, vol. 48, no. 4, pp. 712-717, April 2000.
- [13] H. J. Liebe, "Modeling attenuation and phase of radio wave in air at frequencies below 1000 GHz," *Radio Science*, vol. 16, no. 6, pp. 1183-1199, 1981.
- [14] B. L. Ulich, "Improved Correction for Millimeter-Wavelength Atmospheric Attenuation", *Astrophysical Letters*, vol. 21., pp. 21-28, 1980.
- [15] M. A. Holdaway and J. R. Pardo, "Modeling of the submillimeter Opacity on Chajnantor", NRAO MMA Memo 187, USA, 1997.
- [16] E. Grossman, "AT, atmospheric transmission software user's manual", Airhead Software Cp., Boulder, CO, USA, 1989.
- [17] R. Winston and W. T. Welford, "Design of nonimaging concentrators as second stages in tandem with image-forming first-stage concentrators," *Appl. Opt.*, vol. 19, pp. 347-351, Feb.1980.
- [18] E. W. Weisstein, "Millimeter/submillimeter Fourier transform spectroscopy of jovian planet atmospheres," Doctoral Thesis, California Institute of Technology, Pasadena, California, 1996.
- [19] P. Kaufmann, J. E. R. Costa, C. G. de Castro, Y. R. Hadano, J. S. Kingsley, R. K. Kingsley, H. Levato, A. Marun, J. P. Raulin, M. Rovira, E. Correia, V. R. Silva, "The New Submillimeter-wave Solar Telescope", *Proc. SMBO/IEEE MTT-S International Microwave and Optoelectronics Conference*, August 6-10, Belém, PA, Brasil, 439, 2001.
- [20] A. M. Melo; C. G. Giménez de Castro; P. Kaufmann; H. Levato; A. Marun; P. Pereyra and J. P. Raulin, "Determination of submillimeter atmospheric opacity at El Leoncito, Argentina Andes", *Telecomunicações INATEL*, vol. 6, pp. 32-36, 2003.
- [21] P. Kaufmann; C. G. Giménez de Castro; J. P. Raulin, A. M. Melo; H. Levato; A. Marun; J. L. Giuliani and P. Pereyra, "Comparison of Radiometric Methods for Measuring Atmospheric Transmission at Submillimeter Wavelengths", in preparation, 2003.